Giftet Inc.
Journal of Geolocation, Geo-information, and Geo-intelligence
Volume 2022, article ID 2022071601, 13 pages
https://doi.org/10.18610/JG3.2022.071601

Research Article

Landmark Computation of the Generalized Bessel Function Distributions of the First Kind: Part 1

To my mom, Lumturi Progri: daughter, sister, wife, worker, artisan pizza maker, craftswoman, friend, grandmother, great-grandmother, the best woman I have ever known.

—Ilir F. Progri

Ilir F. Progri
Giftet Inc., 5 Euclid Ave. #3, Worcester, MA 01610, USA
ORCID: 0000-0001-5197-1278
Correspondence should be addressed to Ilir Progri; iprogri@giftet.com

Received May 13, 2022; Revised May 14, 2022-June 17, 2022, Accepted July 16, 2022; Published November 1, 2022.

Scientific Editor-in-Chief/Editor: Ilir F. Progri

Copyright © 2022 Giftet Inc. All rights reserved. This work may not be translated or copied in whole or in part without written permission to the publisher (Giftet Inc., 5 Euclid Ave. #3, Worcester, MA 01610, USA), except for brief excerpts in connection with reviews or scholarly analysis. Use in connection with any form of information storage and retrieval, electronic adaptation, computer software or by similar or dissimilar methodology now known or hereafter developed is forbidden. The use of the publication of trade names, trademarks, service marks, or similar terms, even if they are not identified as such, is not to be taken as an expression of opinion as to whether or not they are subject to proprietary rights.

The landmark computation of the generalized Bessel function distribution of the first kind (GBFD1K) is its first most efficient computation for values of the variable greater than zero and for integer values of another parameter. The GBFD1K is split into two segments from zero to a parameter greater than zero and from that parameter greater than zero to infinity. The parameter that is greater than zero is typically one or two orders of magnitude smaller than one. The efficient computation of the GBFD1K for the first segment is performed using any of the formulae already developed earlier in Progri 2016 and 2018. The landmark computation of the second segment takes advantage of a cleaver substitution that leads to the computation of the Progri L function for the integer values of another parameter. In order to compare and contrast the first landmark computation with the other efficient computation of the GBFD1K a significant improvement of the latter was employed making use of the properties of the exponential and logarithmic functions. According to the numerical results derived for each case to validate the theoretical models presented in the paper, the first landmark computation is from two to several orders of magnitude faster and two to four orders of magnitude more accurate than the efficient computation of GBFD1K for integer values of another parameter. This paper contains a wealth of computation wisdom and knowledge that was generated from the assessment of this problem during the last few years.

Index Terms—Bessel functions, modified Bessel functions, cumulative distribution function, Kampé de Fériet function, Progri L function, incomplete gamma functions, hypergeometric series, landmark computation.

1 Introduction

The discovery of the first landmark computation of the generalized Bessel function cumulative distribution functions (cdf) of the first kind (GBFD1K) for integer values of the parameter p did neither happen by accident nor did it occur immediately. From Progri (2016, [1]) until Progri (2021, [12]) there is a total of twelve journal papers that I developed in the past six years in which I have accumulated a wealth of computational wisdom and knowledge.

What does this computational wisdom and knowledge consist of?

I have exhausted the computation of the Kampé de Fériet function (or double hypergeometric series [1]-[12]) in MATLAB. The work on the computational wisdom and knowledge on the expansion of the efficient computation of the GBFD1K for integer values of the parameter p gave me understanding that its expansion via the Kampé de Fériet function (or double hypergeometric series [1]-[12]) has certain limitations.

The first limitation had to do with the computation of the asymptotic (or the tale) of the distribution. In order to accomplish the above I had to perform a series of improvements of the computation of the Kampé de Fériet function that are discussed in the Sect. 2. As we shall see in Sect. 4, this approach is really not computationally efficient after all for large values of the variable x and for values of the parameter p. I exhausted all the computational improvements came to the realization that equations derived from Progri (2016, [1]) and Progri (2018, [5]) are only useful for small values of the variable x; i.e., $0 < x \leq b$; for $b \ll 1$. A discussion for the value of b in given in Sects. 3 and 4. The main reason is very simply to understand. Equations in Progri (2016, [1]) and Progri (2018, [5]) were really meant to be employed for those values of the variable x. It is only after a lot of computational wisdom and knowledge that I discovered this truth.

It was not easy to come to this realization. It took a lot of computational work that gave me more tools and perfected my prediction and the ability to reason based on the numerical results. Further details of how I came to this realization are given in Sects. 2 and 4.

The beginning of the landmark computation of the GBFD1K started when I came to the realization that what I had done in the past was not nearly enough to meet the performance and speed criteria.

The lack of computational power in both performance and speed had nothing to do with the direct computation of the Kampé de Fériet function (or there had to be a way to reduce the direct computation of the Kampé de Fériet function); because it was not meant to be employed for those values of the variable $b \leq x < \infty$, which I recently discovered after several years of research and development.

It is also important to give a little bit of an analogy as to the scope of the effectiveness of a formula. Imagine being seated in the car and you look at the outside world from several angles. What is in front of you, you can see it from yourself through the windshield. What is on the side, perhaps if you have good eyes, you can see it via your peripheral vision. However, what is behind you, the driver can only see it via a set of mirrors or other sensors. The way the mirrors are set up, is that they can only allow the driver to see a particular angle of the outside world.

The same thing can be said about the formulae that I derived from the efficient computation of GBFD1K in Progri (2016, [1]) and Progri (2018, [5]). These formulae, although very useful, they are only meant to give me a particular view of the solution. I regret that it took me so long to discover the limitation of the solution given in Progri (2016, [1]) and Progri (2018, [5]).

The first landmark computation of GBFD1K is the another mirror that I needed to imagine (i.e., visualize), analytically implement that produce the solution that meets the criteria in both computational accuracy, performance, and speed. Furthermore, analytical, technical details of how I came about to produce the first landmark computation of GBFD1K are given in Sects. 3 and 4. In Progri (2016, [3]), I produced two formulas side by side. The key to the first landmark computation of GBFD1K was on Sect. 3, pg. 56 of Progri (2016, [3]). Once, I realized what was needed to derive the solution of the first landmark computation of the GBFD1K, I knew where to look. It was something that I thought about it all along. I probably did not give myself a lot of credit for its derivation back then. The first landmark computation of the GBFD1K is made possible via the Progri L^{i} function.

This paper is organized as follows: in Sect. 2 asymptotic computation of the GBFD1K is discussed. The first landmark computation of the GBFD1K is presented in Sect. 3. Section 4 contains numerical, theoretical results; Conclusion is provided in Sect. 5 along with a list of references. In Appendix A: A super-efficient implementation of incomplete gamma function is presented.

2 Asymptotic Computation of the GBFD1K

The closed form expressions of the GBFD1K cdf in Progri (2016, [1]) (117) and Progri (2018, [5]) (23)-(25), (49)-(51) were not tested for large value of the variable x; i.e., the asymptotic behavior for these formulae was unknown.

There were two questions that needed to be answered. The first question was as follows:

What modifications of the equations in Progri (2016, [1]) and Progri (2018, [5]) are needed to enable the efficient computation of the GBFD1K?

Two major modifications of the equations derived in Progri (2016, [1]) and Progri (2018, [5]) were performed to enable the asymptotic efficient computation of the GBFD1K.

First, in Progri (2016, [1]) (117) we have the closed form expression of the GBFD1K cdf as given below

$$F_{\text{GBessel1}}(x;a,d,p)=\frac{(d^2-1)^{p_1}e^{-dx}x^{2p_1}\left(K_1+\frac{dx}{2p_2}K_2\right)}{\Gamma(2p_2)}$$

$$=\frac{C_{11}(d,p)x^{2p_1}\left[K_1(x)+\frac{dx}{2p_2}K_2(x)\right]}{e^{dx}}$$

$$=C_{11}(d,p)e^{-dx}x^{2p_1}K(x,d,p) \tag{1}$$

where, $C_{11}(d,p)$ is given by Progri (2016, [1]) (118) and Progri (2018, [5]) (26) $K_1(x)$, $K_2(x)$ are known as the Kampé de Fériet functions

$$K_1(x)=F^{0:1;1}_{2:0;0}\left[\begin{matrix}-:p_1;1;\\ p_3,p_2:-;-;\end{matrix}x_1,x_2\right]$$

$$=\sum_{k,m=0}^{\infty}k^{1,2}_{1k,m}(x)$$

$$=\sum_{k,m=0}^{\infty}\frac{(p_1)_k(1)_m}{(p_3)_{m+k}(p_2)_{m+k}}\frac{(x_1)^k}{k!}\frac{(x_2)^m}{m!} \tag{2}$$

$$K_2(x)=F^{0:1;1}_{2:0;0}\left[\begin{matrix}-:p_1;1;\\ p_4,p_3:-;-;\end{matrix}x_1,x_2\right]$$

$$=\sum_{k,m=0}^{\infty}k^{1,2}_{2k,m}(x)$$

$$=\sum_{k,m=0}^{\infty}\frac{(p_1)_k(1)_m}{(p_4)_{m+k}(p_3)_{m+k}}\frac{(x_1)^k}{k!}\frac{(x_2)^m}{m!} \tag{3}$$

Next, we will utilize the identity for $\forall x>0$

$$x\equiv e^{\log(x)} \tag{4}$$

Taking the log function of (1) produces

$$\log(F)=\log\left[\frac{(d^2-1)^{p_1}e^{-dx}x^{2p_1}\left[K_1(x)+\frac{dx}{2p_2}K_2(x)\right]}{\Gamma(2p_2)}\right]$$

$$=2p_1\log(x)-dx+\log\left[K_1(x)+\frac{dx}{2p_2}K_2(x)\right]+q \tag{5}$$

where

$$q=p_1\log(d^2-1)-\log[\Gamma(2p_2)]$$

$$=\log[C_{11}(d,p)] \tag{6}$$

As $x\to\infty$ then we have

$$\log(F)\to 0 \tag{7}$$

It means that

$$\log\left[K_1(x)+\frac{dx}{2p_2}K_2(x)\right]\to dx-2p_1\log(x)-q \tag{8}$$

Second, we have to ensure that the inside terms of the Kampé de Fériet functions $K_1(x)$, $K_2(x)$ do not blow up.

$$k^{1,2}_{1k,m}(x)=\frac{(p_1)_k(1)_m}{(p_3)_{m+k}(p_2)_{m+k}}\frac{(x_1)^k}{k!}\frac{(x_2)^m}{m!}$$

$$=e^{\log\left[\frac{(p_1)_k(1)_m}{(p_3)_{m+k}(p_2)_{m+k}}\frac{(x_1)^k(x_2)^m}{k!\quad m!}\right]}\text{[ii]} \tag{9}$$

The advantage of (9) is that it will reduce the product into a summation or difference of logs. But nevertheless, we will still have to take the exponential function in the end. As seen in (9), for large values of x_1 and x_2 and for large number of terms, the Kampé de Fériet functions $K_1(x)$, $K_2(x)$ will be quite large; hence, the computational error for computing the asymptotic behavior of equations in Progri (2016, [1]) (117) and Progri (2018, [5]) (23)-(25), (49)-(51) is expected to grow exponentially with the increase of the variable x.

Now, having computed the asymptotic behavior of equations in Progri (2016, [1]) (117) and Progri (2018, [5]) (23)-(25), (49)-(51) we have arrived at the second question?

Are these equations intended to compute the asymptotic behavior of the GBFD1K?

Based on the analytical and numerical results in Sect. 4, the answer to the second question is an emphatic NO.

The reason why the answer to this question is an emphatic NO is because as we shall see in Sect. 4 for large values of x these equations will produce more computational error and will take a lot longer to compute.

This concludes the discussion on the asymptotic behavior of the computation of the GBFD1K cdf.

3 Landmark[iii] Computation of the GBFD1K

Although in Sect. 2 I came to the realization that equations in both Progri (2016, [1]) (117) and Progri (2018, [5]) (23)-(25), (49)-(51) are really not meant for large values of the variable x; in all fairness, they appear to be working just fine for small values of the variable x.

Therefore, in all fairness, in framing the landmark computation of the GBFD1K cdf, I had a lot to begin with: I was absolutely convinced that these equations worked perfectly fine for small values of the variable x; however, modifications were required for large values of the variable x and integer values of the parameter p. In addition, in the past I also had performed a substitution in Progri (2018, Sect. 3 pg. 56 [3]) that was intended for precisely what was needed.

All was left to do is assembling (or creating), which is exactly what is performed in the remainder of this section.

In Progri (2016, [1] (80)) the GBFD1K cdf is given by.

$$F_{\text{GBessel1}}(x;a,d,p)=\frac{1}{C_1(p,d)}\sum_{k=0}^{\infty}\frac{\int_0^x t^{2p+2k}e^{-td}dt}{k!\Gamma(p_2+k)2^{p+2k}} \tag{10}$$

From this expression we have derived two alternative computations of the GBFD1K cdf in Progri (2018, [5] (23) and (49)). These expressions work well for small values of x. However, Progri (2018, [5] (49)) becomes unstable (or diverges) rather for larger values of x. We know that this integral should not diverge. The only way to resolve the divergence is my means of a transformation[iv].

For values of $x \geq b$, (10) can be written as

$$F_{\text{GBessel1}}(x;a,d,p)=\frac{\sum_{k=0}^{\infty}\frac{\int_0^b t^{2p+2k}e^{-td}dt+\int_b^x t^{2p+2k}e^{-td}dt}{k!\Gamma(p_2+k)2^{p+2k}}}{C_1(p,d)}$$

$$=\left|\begin{array}{l}\dfrac{\sum_{k=0}^{\infty}\frac{\int_0^b t^{2p+2k}e^{-td}dt}{k!\Gamma(p_2+k)2^{p+2k}}}{C_1(p,d)}\\ +\dfrac{\sum_{k=0}^{\infty}\frac{\int_b^x t^{2p+2k}e^{-td}dt}{k!\Gamma(p_2+k)2^{p+2k}}}{C_1(p,d)}\end{array}\right.$$

$$=\left|\begin{array}{l}F_{\text{GBessel1}}(x=b;a,d,p)\\ +\dfrac{\sum_{k=0}^{\infty}\frac{\int_b^x t^{2p+2k}e^{-td}dt}{k!\Gamma(p_2+k)2^{p+2k}}}{C_1(p,d)}\end{array}\right. \tag{11}$$

If we make the substitution (see Progri (2018, Sect. 3 pg. 56 [3])) for calculating (10) for values of $x \geq b$ we have the following

$$t'=e^{-td} \Rightarrow t=\frac{\log(t')}{-d} \Rightarrow dt=-\frac{dt'}{t'd} \tag{12}$$

When

$$t \to |_b^x \Rightarrow t' \to |_{e^{-bd}}^{e^{-xd}} \tag{13}$$

Substituting (12) and (13) into the integral of (11) yields

$$\int_b^x t^{2p+2k}e^{-td}dt=\frac{\int_{e^{-xd}}^{e^{-bd}}\log^{2p+2k}(t')dt'}{d^{2p+2k+1}} \tag{14}$$

Where

$$\alpha=2p+2k \tag{15}$$

$$\alpha'=(2p+1\equiv 2p_1)+2k \tag{16}$$

The solution of (16) can be obtained from Gradshteyn, Ryzhik (2007, 2.71, 2.711 pg. 237 [25]) as follows

$$\int_b^x t^{\alpha}e^{-td}dt=\frac{\int_{e^{-xd}}^{e^{-bd}}\log^{\alpha}(t')dt'}{d^{\alpha'}}\ [\text{v}]$$

$$=\frac{\sum_{n=0}^{\alpha}(-1)^{n-\alpha}\alpha(\alpha-1)\cdots(\alpha-n+1)t'\log^{\alpha-n}(t')|_{e^{-xd}}^{e^{-bd}}}{d^{\alpha'}}\ [\text{vi}]$$

$$=\frac{\sum_{n=0}^{\alpha}(-1)^{n-\alpha}\alpha(\alpha-1)\cdots(\alpha-n+1)\left[\frac{\log^{\alpha-n}(e^{-bd})}{e^{bd}}-\frac{\log^{\alpha-n}(e^{-xd})}{e^{xd}}\right]}{d^{\alpha'}}$$

$$=\frac{\sum_{n=0}^{\alpha}(-1)^{n-\alpha}\alpha(\alpha-1)\cdots(\alpha-n+1)\left[e^{-bd}(-d)^{\alpha-n}-e^{-xd}(-xd)^{\alpha-n}\right]}{d^{\alpha'}}$$

$$=\frac{\sum_{n=0}^{\alpha}\alpha(\alpha-1)\cdots(\alpha-n+1)\left(e^{-bd}b^{\alpha-n}-e^{-xd}x^{\alpha-n}\right)d^{-n}}{d}$$

$$=\frac{\sum_{n=0}^{\alpha}\binom{\alpha}{n}n!\left(e^{-bd}b^{\alpha-n}-e^{-xd}x^{\alpha-n}\right)d^{-n}}{d}$$

$$=\frac{e^{-bd}b^{\alpha}\sum_{n=0}^{\alpha}\binom{\alpha}{n}n!b^{-n}d^{-n}-e^{-xd}x^{\alpha}\sum_{n=0}^{\alpha}\binom{\alpha}{n}n!x^{-n}d^{-n}}{d}\ [\text{vii}] \tag{17}$$

Substituting (17) into (11) produces

$$\Delta F_{\text{GBessel1}}(x\geq b;a,d,p)=\frac{L(x,b,d,p)\,[\text{viii}]}{C_1(d,p)}$$

$$=C_{11}(d,p)L(x,b,d,p) \tag{18}$$

where Progri $L(x,b,d,p)$ function is defined for values of the variable $x \geq b$ and integer values of the parameter p as

$$L(x,b,d,p)=\frac{2p_1\sum_{k=0}^{\infty}\frac{\frac{1}{2^{2k}}\frac{\left|\begin{array}{l}e^{-bd}b^{\alpha}\sum_{n=0}^{\alpha}\binom{\alpha}{n}nb^{-n}d^{-n}\\ -e^{-xd}x^{\alpha}\sum_{n=0}^{\alpha}\binom{\alpha}{n}nx^{-n}d^{-n}\end{array}\right.}{d}}{(p_2)_k k!}}{\Gamma(p_2)} \tag{19}$$

It is straightforward to see that for $x=b$ then (18) is equal to zero because in (19) the Progri $L(x,b,d,p)$ vanishes as follows

$$\Delta F_{\text{GBessel1}}(x=b;a,d,p)=\frac{L(x=b,b,,d,p)}{C_1(d,p)}=0 \tag{20}$$

However, when $x \to \infty$

$$L(x \to \infty, b, d, p) = \frac{2p_1 e^{-bd} b^{\alpha} \sum_{k=0}^{\infty} \frac{\frac{1}{2^{2k}}}{(p_2)_k k!} \sum_{n=0}^{\alpha} \frac{\binom{\alpha}{n} n}{b^n d^n}}{\mathrm{d}\Gamma(p_2)} \tag{21}$$

The first landmark computation of the GBFD1K cdf which can be written with the help of Progri $L(x, b, d, p)$ is supported from the numerical, theoretical results in Sect. 4; therefore, this solution is meant for values of the variable $(b \ll 1) \leq x < \infty$. Why? For two main reasons.

First, the first landmark solution does not diverge as the variable x increases; i.e., regardless of how large the value of the variable x the accuracy or the numerical error is independent of the value of the variable x and the number of terms, N.

Second, the computational complexity of the first landmark cdf given by (18) is on the order of $O(N\mathrm{Log}N)$; hence, the landmark computation of the GBFD1K cdf is expected to be very fast, much faster than the efficient computation will ever be as explained later in the remainder of the section.

Finally, if we substitute (21) in (11) we have the complete landmark solution of the GBFD1K cdf integer values of the parameter p is extracted as follows:

$$F_{\mathrm{GBessel1}}(x; a, d, p) = \frac{\left| \begin{array}{ll} \frac{x^{2p_1}\left[K_1(x) + \frac{dx}{2p_2} K_2(x)\right]}{e^{dx}} & 0<x\leq b \\ \frac{K_1(b) + \frac{dx}{2p_2} K_2(b)}{b^{-2p_1} e^{db}} + L(x,b,d,p) & b\leq x<\infty \end{array} \right.}{C_{11}^{-1}(d,p)} \tag{22}$$

or

$$F_{\mathrm{GBessel1}}(x; a, d, p) = \frac{\left| \begin{array}{ll} x^{2p_1}\left[K_3(x) - \frac{p_1 dx}{p_2} K_4(x)\right] & 0<x\leq b \\ \frac{K_3(b) - \frac{p_1 db}{p_2} K_4(b)}{b^{-2p_1}} + L(x,b,d,p) & b\leq x<\infty \end{array} \right.}{C_{11}^{-1}(d,p)} \tag{23}$$

Where from Progri (2018, [5]) (49) we have the Kampé de Fériet functions $K_3(x)$, $K_4(x)$ as follows

$$\begin{aligned} K_3(x) &= \sum_{k,m=0}^{\infty} \frac{(p_1)_{k+m}}{(p_3)_{m+k}(p_2)_k\left(\frac{1}{2}\right)_m} \frac{(x_1)^k}{k!} \frac{(x_2)^m}{m!} \\ &= F_{1:1;1}^{1:0;0}\left[\begin{matrix} p_1: -; -; \\ p_3: p_2; \frac{1}{2}; \end{matrix} x_1, x_2\right] \end{aligned} \tag{24}$$

$$\begin{aligned} K_4(x) &= \sum_{k,m=0}^{\infty} \frac{(p_2)_{k+m}}{(p_4)_{m+k}(p_2)_k\left(\frac{3}{2}\right)_m} \frac{(x_1)^k}{k!} \frac{(x_2)^m}{m!} \\ &= F_{1:1;1}^{1:0;0}\left[\begin{matrix} p_2: -; -; \\ p_4: p_2; \frac{3}{2}; \end{matrix} x_1, x_2\right] \end{aligned} \tag{25}$$

Typically, the value of the parameter b are as follows:

$$0 < b \ll 1 \tag{26}$$

This concludes the discussion on the landmark computation of the of the GBFD1K cdf.

4 Numerical, Theoretical Results

There is a lot that was accomplished since the last numerical, theoretical results in Progri (2018, [5]).

Moreover, there are several journal papers that discuss the simulation test setup from Progri (2016, [1]) to Progri (2021, [12]).

The main purpose of the simulation results in this journal paper is to illustrate either the significant improvements or shortcoming in both performance and speed of the Progri (2016, [1]) and Progri (2018, [5]) that were obtained as a result of the asymptotic behavior of the computation of the GBFD1K cdf and then to compare and contrast with the landmark computation of the GBFD1K cdf for integer values of the parameter, p.

4.1 Asymptotic vs. Alternate Computation of the GBFD1K

In this subsection we present the simulation results due to either the significant improvements or shortcoming in both performance and speed of the Progri (2016, [1]) and Progri (2018, [5]) that were obtained as a result of the asymptotic behavior of the computation of the GBFD1K cdf.

Figure 1(a) shows the plots of (top) the GBFD1K pdf and cdf for $a = 1$, $d = 2$, and $p = 1$, $0 \leq x \leq 2$ and $N = 30$ for the integral, cdf1, and linear numerical approximation, cdf2; (bottom) cdf using Progri (2016, [1]) (116) or (117) and Progri (2018, [5]) (25) cdf3 and (49) cdf4. Since, there are four different options for computing the Kampé de Fériet functions, for this simulation test setup, we were able to achieve exactly the same performance for either one of the options.

Figure 1(b) shows the absolute error of the GBFD1K cdf for (top) the integral minus the linear numerical approximation and (bottom) integral minus the Progri (2018, [5]) (25) and (49).

For a small region of the variable $0 \leq x \leq 2$; cdf3 Progri (2018, [5]) (25) and cdf4 Progri (2018, [5]) (49) produce very good performance results up to fourteen orders of magnitude accuracy compared to the integral solution cdf1. Nevertheless, we notice that cdf4 appears to diverge rapidly.

We repeat the same setup in Figs. 2(a) and (b) for the variable $0 \leq x \leq 10$, $N = 70$, and for opts. 1 and 2 of the Kampé de Fériet functions. We notice a significant reduction in performance of the cdf4. Figures 3(a) and (b) are the same of Figs. 2(a) and (b) for opts. 3 and 4 of the Kampé de Fériet functions. Because cdf4 is diverging, opts. 3 and 4 will make it worse.

Based on these calculations alone we conclude that cdf4 Progri (2018, [5]) (49) is really meant to be employed in this form for $0 \leq x \ll 1$. The performance of Progri (2018, [5]) (25) cdf3 remains to be compared and contrasted with (22) which is accomplished in the following section.

4.2 *Asymptotic vs. First Landmark Computation of the GBFD1K*

From Subsect. 4.1 we were able to assess that Progri (2018, [5]) (25) (49) cdf4 should not be employed in the current form for computing GBFD1K cdf for integer values of p. Instead in this subsection we compare and contrast cdf3 given by Progri (2018, [5]) (25) and cdf4 given by (22).

In Figs. 4(a)-(e) we repeat the same setup as in previous figures for $a = 1,\ d = 2$, and $p = 1,\ 0 \leq x \leq 200$.

Figure 4(b) corresponds to absolute error of the integral minus the Progri (2018, [5]) (25) $N = 100$ opt. 1 for computing the Kampé de Fériet functions and landmark (22) and $N = 30$ and opt. 1 for computing the Progri L function. In Fig. 4(c) same as 4(b) for opt. 2 for computing the Kampé de Fériet functions and opt. 2 for computing the Progri L function. Ditto for Fig. 4(d) $N = 150$ and opt. 3 for computing the Kampé de Fériet functions and opt. 3 for computing the Progri L function. Finally, Ditto for Fig. 4(e) $N = 270$ and opt. 4 for computing the Kampé de Fériet functions and opt. 4 for computing the Progri L function.

Based the simulation results from Figs. 4(a)-(e), the asymptotic computation of the GBFD1K cdf as discussed in Sect. 2 can only work for a large number of terms and only for opt. 4 opt. 4 for computing the Kampé de Fériet functions.

We conclude that in the current form Progri (2018, [5]) (25) is not an efficient computation of the GBFD1K cdf for larger values of the variable x.

Finally, it remains to assess the performance of the landmark (22) vs landmark (23) which is considered and articulated in the following subsection.

4.3 *Landmark vs. Landmark Computation of the GBFD1K*

From Subsect. 4.2 we were able to assess that Progri (2018, [5]) (25) (25) cdf3 should not be employed in the current form. Instead in this subsection we compare and contrast cdf3 given by (22) and cdf4 given by (23) for various options for computing the Progri L function.

In Figs. 5(a)-(e) we repeat the same setup as in previous figures for $a = 1,\ b = 0.1\ d = 2$, and $p = 1,\ 0 \leq x \leq 200$.

Figure 5(b) corresponds to absolute error of the integral, cdf1, minus landmark (22), cdf3, and landmark (23), cdf4, and $N = 30$ and opt. 1 for computing the Progri L function. In Fig. 5(c) same as 5(b) for opt. 2 opt. 2 for computing the Progri L function. Ditto for Fig. 5(d) opt. 3 for computing the Progri L function. Finally, Ditto for Fig. 5(e) opt. 4 for computing the Progri L function.

Based the simulation results from Figs. 5(a)-(e), the landmark computation of the GBFD1K as discussed in Sect. 3 works extremely well for large values of the variable $x \gg 1$ for small number of terms for computing the Progri L and regardless of the option that is used for computing the Progri L.

We conclude that the landmark solution (22) or (23) is definitely a landmark computation of the GBFD1K for larger values of the variable x and for integer values of the parameter p.

5 Conclusions

We performed a thorough investigation of the GBFD1K cdf from Progri (2016, [1]) and Progri (2018, [5]) based on the body of wisdom and knowledge accumulated in the past six years from Progri (2016, [1]) until Progri (2021, [12]).

We found that for integer values of the parameter p and for large values of the variable x the closed form expressions of the GBFD1K from Progri (2016, [1]) and Progri (2018, [5]) are very inefficient. These equations were only intended for small values of the variable x as shown in Figs 1-5 and Tab. I.

For large values of the variable x and for integer values of the parameter p, we derived the first landmark solution of the GBFD1K cdf.

Based on the performance speed from Tab. I, the first landmark solution of the GBFD1K cdf appears to be two orders of magnitude faster than the integral solution and four orders of magnitude faster than the asymptotic solution.

6 Acknowledgement

This work was supported by Giftet Inc. executive office.

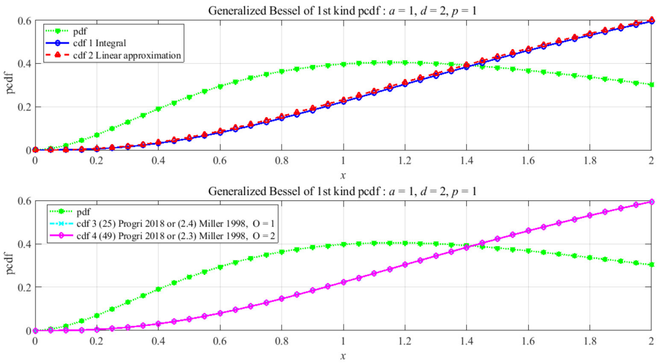

(a) (top) GBFD1K pdf and cdf for $a = 1$, $d = 2$, and $p = 1$, $0 \leq x \leq 2$ for the integral and linear numerical approximation; (bottom) GBFD1K pdf and cdf for Progri (2016, [1]) (116) or (117) and Progri (2018, [5]) (25) and (49) and $N = 30$.

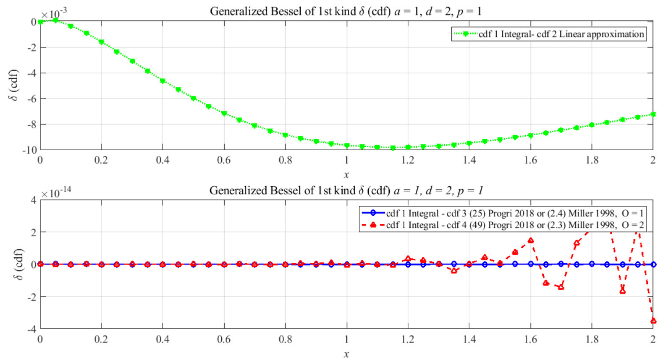

(b) absolute error of the GBFD1K same as (a) for (top) the integral minus the linear numerical approximation; (bottom) integral minus the Progri (2018, [5]) (25) and (49).

FIGURE 1: Numerical calculations of the (a) GBFD1K pdf and cdf vs. (b) the absolute error: original pdf and cdf: p an integer based on the computation of Kampé de Fériet function.

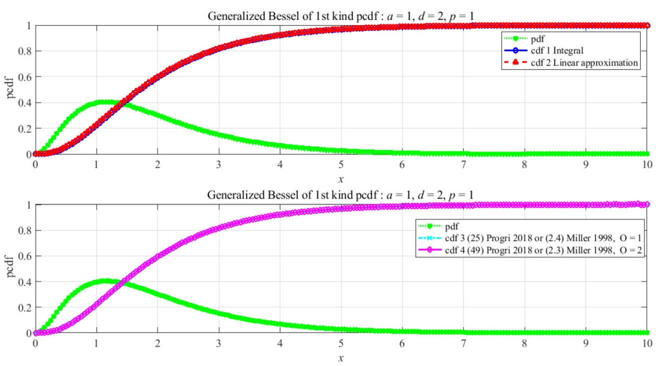

(a) (top) GBFD1K pdf and cdf for $a = 1$, $d = 2$, and $p = 1$, $0 \leq x \leq 10$ for the integral and linear numerical approximation; (bottom) original GBFD1K pdf and cdf for Progri (2016, [1]) (116) or (117) and Progri (2018, [5]) (25) and (49) and $N = 70$.

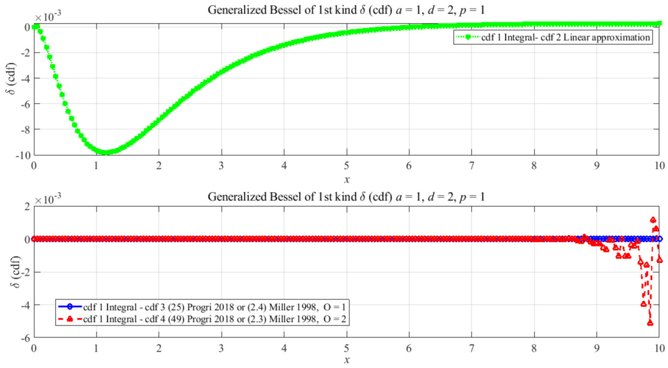

(b) absolute error of the GBFD1K same as (a) for (top) the integral minus the linear numerical approximation; (bottom) integral minus the Progri (2018, [5]) (25) and (49).

FIGURE 2: Numerical calculations of the absolute error of the GBFD1K pdf and cdf same as Fig. 1 for $0 \leq x \leq 10$ and for options 1 and 2 for computing the Kampé de Fériet functions.

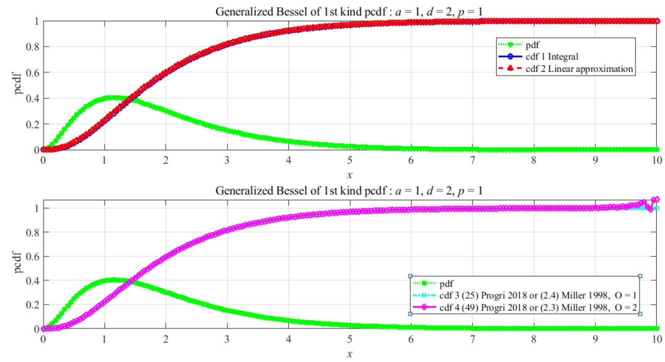

(a) (top) GBFD1K pdf and cdf for $a = 1$, $d = 2$, and $p = 1$, $0 \leq x \leq 10$ for the integral and linear numerical approximation; (bottom) GBFD1K pdf and cdf for Progri (2016, [1]) (116) or (117) and Progri (2018, [5]) (25) and (49) and $N = 70$.

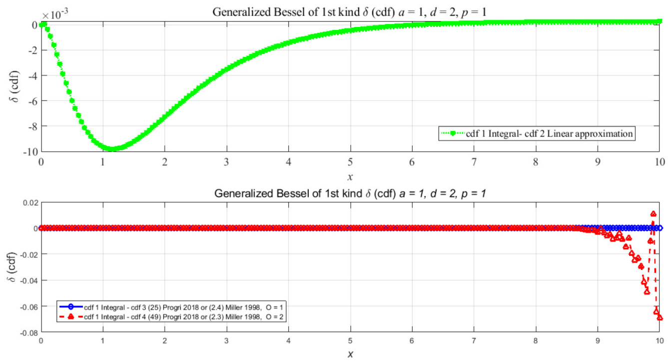

(b) absolute error of the GBFD1K same as (a) for (top) the integral minus the linear numerical approximation; (bottom) integral minus the Progri (2018, [5]) (25) and (49).

FIGURE 3: Numerical calculations of the absolute error of GBFD1K pdf and cdf same as Fig. 2 but for options 3 and 4 for computing the Kampé de Fériet functions.

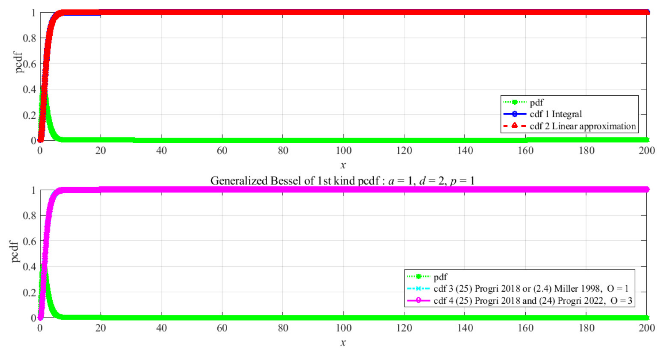

(a) same as 2 (a) (top) $0 \leq x \leq 200$ the integral, cdf1, and linear numerical approximation, cdf2; (bottom) GBFD1K pdf and cdf for Progri (2018, [5]) (25), cdf3, $N = 100$ opt. 1 for computing the Kampé de Fériet functions and landmark (22), cdf4, and $N = 30$ and opt. 1 for computing the Progri L function.

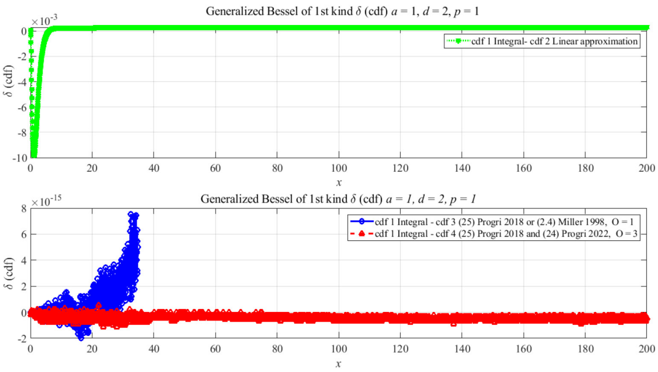

(b) absolute error of the GBFD1K same as (a) opt. 1.

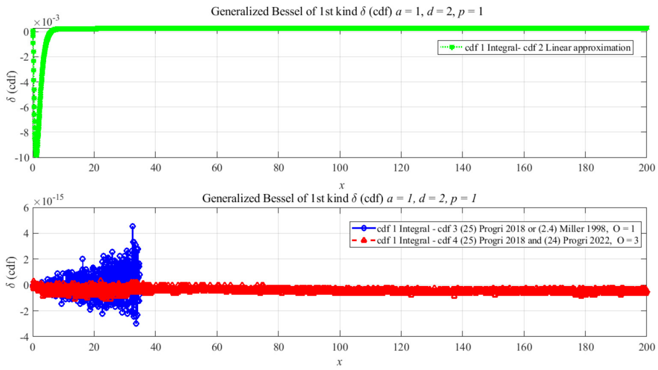

(c) same as (b) opt. 2.

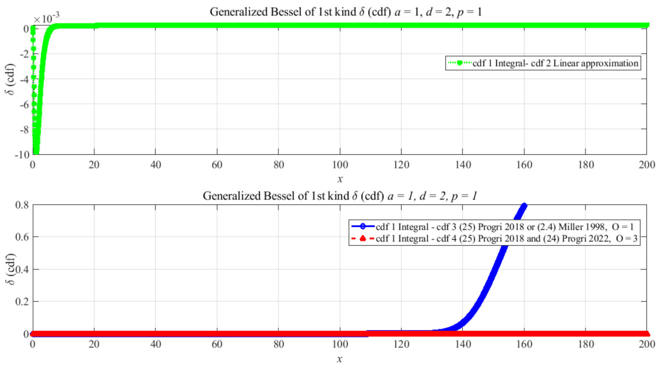

(d) same as (b) $N = 150$ opt. 3 and opt. 3.

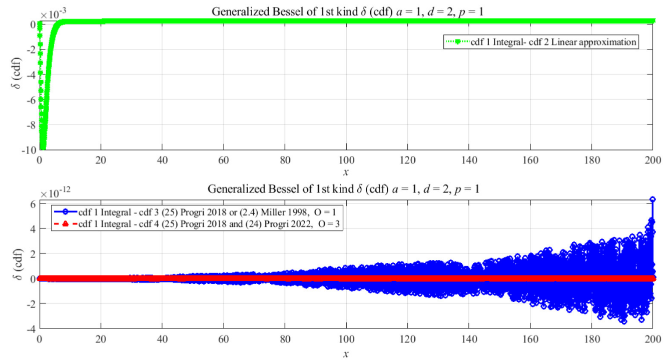

(e) same as (b) $N = 270$ opt. 4 for computing the Kampé de Fériet functions and opt. 4 for computing the Progri L function.

FIGURE 4: Numerical calculations the GBFD1K pdf and cdf and the absolute error of the landmark cdf.

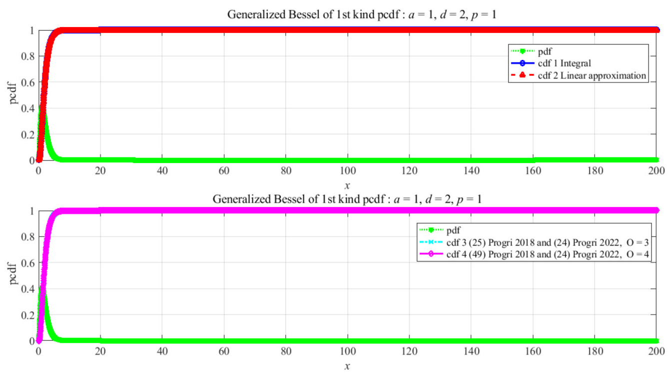

(a) same as 4(a) (top); (bottom) original GBFD1K pdf and cdf landmark (22), cdf3, landmark (23), cdf4, and $N = 30$ and opt. 1 for computing the Progri L function.

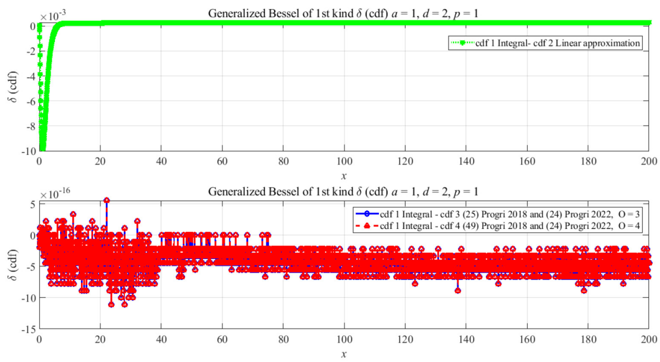

(b) same as 4(b).

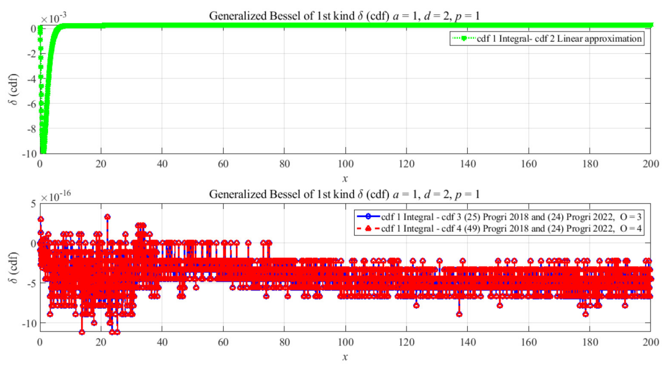

(c) same as (b) opt. 2 for computing the Progri L function.

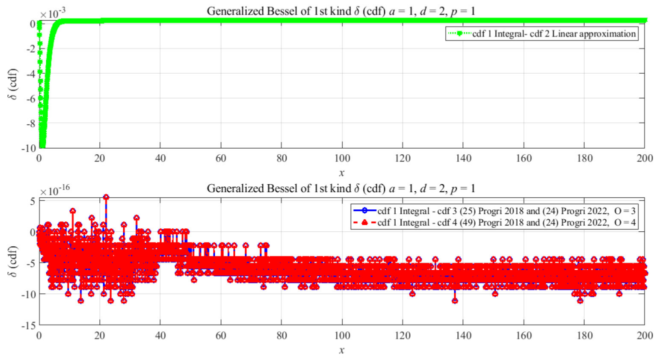

(d) same as (b) opt.3 for computing the Progri L function.

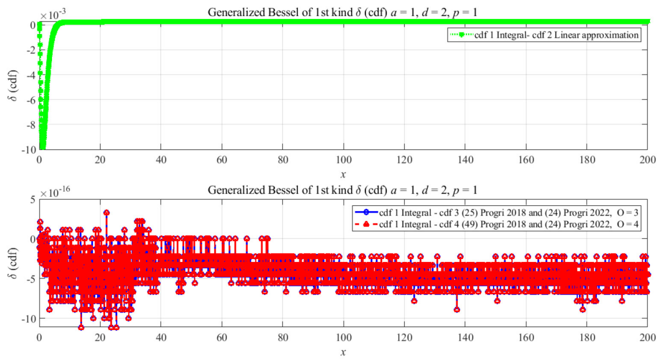

(e) same as (b) opt.4 for computing the Progri L function.

FIGURE 5: Numerical calculations GBFD1K pdf and cdf and the absolute error of the landmark cdf.

TABLE I: THE QUANTITATIVE COMPUTATIONAL PERFORMANCE

GBFD1K cdf: CFE 1 Int; CDF2 LA; CDF (25) vs. CFE 4 (49) $a=1,\ d=2,\ p=1,\ 0\le x\le 2\quad \sum(\cdot)=30$ terms			
Integral (ms)	L. Ap. (ms)	CFE 3 (ms)	CFE 4 (ms)
13.8	0.1	91.6	84.1 Op 1
15.6	<<0.1	1718	231. Op 2
13.8	<<0.1	28.5	31.9 Op 3
13.3	<<0.1	21.4	23.9 Op 4
CFE 1 Int; CDF2 LA; CDF 3 (25) vs. CFE 4 (49) $a=1,\ d=2,\ p=1,\ 0\le x\le 10\quad \sum(\cdot)=70$ terms			
(ms)	(ms)	(sec)	(sec)
96.5	<<0.1	0.474	0.458 Op 1
80.7	<<0.1	1.723	2.502 Op 2
79.2	<<0.1	0.208	0.208 Op 3
80.3	<<0.1	0.193	0.198 Op 4
CFE 1 Int; CDF2 LA; CDF 3 (25) vs. CFE 4 (22) $a=1,\ d=2,\ p=1,\ 0\le x\le 200$ (25) $\sum(\cdot)=270$ terms vs. (22) $\sum(\cdot)=30$			
(sec)	(ms)	(sec)	(sec)
3.039	0.1	16.77	0.580 Op 1
3.031	0.1	93.99	0.428 Op 2
3.011	0.1	24.95	0.027 Op 3
3.017	0.1	25.12	0.039 Op 4
CFE 1 Int; CDF2 LA; CDF 3 (25) vs. CFE 4 (22) $a=1,\ d=2,\ p=1,\ 0\le x\le 200$ (22) $\sum(\cdot)=30$ terms vs. (23) $\sum(\cdot)=30$			
(sec)	(ms)	(sec)	(sec)
3.062	0.1	0.553	0.550 Op 1
3.031	0.1	0.397	0.426 Op 2
3.011	0.1	0.026	0.024 Op 3
3.014	0.1	0.051	0.034 Op 4

I want to profoundly thank the MathWorks at Natick, Massachusetts for providing a sponsored MATLAB licence [29] to Giftet Inc. as part of the Indoor Geolocation Systems MATLAB Library development that will enable the results of this work to be published in Dr. Progri pioneer publication *Indoor Geolocation Systems—Theory and Applications. Vol. I* (Not yet available in print) [24].

This journal paper is dedicated to four special men in my life: my grandfather, Xhevdet Progri, my dear father, Fiqiri Progri, my father's first cousin Dr. Peter Demir, and Qazim Demir, the brother of my grandfather, Xhevdet Progri.

This journal paper is also dedicated to the Golden Bear, Jack Nicklaus, the greatest golfer of all time. Needless, to say I have fallen in love with his masterpiece book, *Golf My Way*. Moreover, Jack Nicklaus [30] reminds me of my grandfather who I loved him very much.

Finally, I am also dedicating this journal paper to our most beloved President Ronald Reagan, who reminds me of my grandfather, [31] who spoke from the heart, who spoke the truth, who was a staunch supporter of personal freedom, the greatest leader of the free world, and perhaps the greatest critic of the wasteful government control and spending[ix].

"*Government is not the answer, government is the problem.*"—Ronald Reagan

I would like to express my deepest gratitude to my mother Lumturi Progri, my sister Adriana Dine, and Ms. Elizabeth Demir for their support, loyally, and dedication to me during some of the most difficult times in my life as a boy, man, and scholar.

7 References

[1] I.F. Progri, "Generalized Bessel function distributions," *J. Geol. Geoinfo. Geointel.*, vol. 2016, article ID

2016071602, 15 pg., Nov. 2016. DOI: https://doi.org/10.18610/JG3.2016.071602

[2] I.F. Progri, "Exponential generalized Beta distribution," *J. Geol. Geoinfo. Geointel.,* vol. 2016, article ID 2016071603, 18 pg., Nov. 2016. DOI: https://doi.org/10.18610/JG3.2016.071603

[3] I.F. Progri, "Hypergeometric function partial derivatives," vol. 2016, article ID 2016071604, 21 pg., Nov. 2016. DOI: https://doi.org/10.18610/JG3.2016.071604

[4] I.F. Progri, "Generalized parabolic cylinder function distribution," vol. 2016, article ID 2016071605, 14 pg., Nov. 2016. DOI: https://doi.org/10.18610/JG3.2016.071605

[5] I.F. Progri, "Efficient computation of generalized Bessel function distributions," *J. Geol. Geoinfo. Geointel.*, vol. 2018, article ID 2018071604, 12 pg., Nov. 2018. DOI: https://doi.org/10.18610/JG3.2018.071605

[6] I.F. Progri, "Efficient computation of the special cases of the generalized Bessel function distributions," *J. Geol. Geoinfo. Geointel.,* vol. 2019, article ID 2019071601, 31 pg., Nov. 2019. DOI: https://doi.org/10.18610/JG3.2019.071601

[7] I.F. Progri, "The computation of a 2F2 hypergeometric function," *J. Geol. Geoinfo. Geointel.,* vol. 2020, article ID 2020071601, 12 pg., Nov. 2020. DOI: https://doi.org/10.18610/JG3.2020.071601

[8] I.F. Progri, "Confluent hypergeometric function irregular singularities," *J. Geol. Geoinfo. Geointel.,* vol. 2021, article ID 2021071601,12 pg., Nov. 2021. DOI: https://doi.org/10.18610/JG3.2021.071601

[9] I.F. Progri, "Efficient computation of the generalized parabolic cylinder function distribution," *J. Geol. Geoinfo. Geointel.,* vol. 2021, article ID 2021071602, 17 pg., Nov. 2021. DOI: https://doi.org/10.18610/JG3.2021.071602

[10] I.F. Progri, "Landmark computation of the generalized parabolic cylinder function distribution," *J. Geol. Geoinfo. Geointel.,* vol. 2021, article ID 2021071603, 15 pg., Nov. 2021. DOI: https://doi.org/10.18610/JG3.2021.071603

[11] I.F. Progri, "Special cases of the generalized parabolic cylinder function distribution," *J. Geol. Geoinfo. Geointel.,* vol. 2021, article ID 2021071604, 12 pg., Nov. 2021. DOI: https://doi.org/10.18610/JG3.2021.071604

[12] I.F. Progri, "The significance of Kampé de Fériet functions in the computation of certain generalized distributions," *J. Geol. Geoinfo. Geointel.,* vol. 2021, article ID 2021071605, 7 pg., Nov. 2021. DOI: https://doi.org/10.18610/JG3.2021.071605

[13] K. Pearson, "Tables of the incomplete gamma-function," Nature, vol. 110, pp 669-, Nov. 1922. DOI: https://doi.org/10.1038/110669c0

[14] A.R., DiDonato, A.H. Morris Jr., "Computation of the incomplete gamma function ratios and their inverse," *ACM Trans. Math. Soft. (TOMS)*, vol. 12, no. 4, pp. 377-393, 1986. DOI: https://doi.org/10.1145/22721.23109

[15] N.M. Temme "Uniform asymptotics for the incomplete gamma functions starting from negative values of the parameters," *Methods & Appl. Analy.* vol. 3, no. 3, pp. 335-344, 1996.

[16] S. Winitzki "Computing the incomplete Gamma function to arbitrary precision." in: V. Kumar, M.L. Gavrilova, C.J.K. Tan, P. L'Ecuyer (eds) *Comp. Science & Appl. — ICCSA 2003*. ICCSA 2003. Lecture Notes in Computer Science, vol. 2667, pp. 790-798. Springer, Berlin, Heidelberg, 2003.

[17] U. Blahak, "Efficient approximation of the incomplete gamma function for use in cloud model applications," *Geoscien. Mod. Devel.*, vol. 3, no. 2, pp. 329-336, Jul. 2010. DOI: https://doi.org/10.5194/gmd-3-329-2010

[18] I. Thompson, "Algorithm 926: Incomplete Gamma functions with negative arguments," *ACM Trans. Math. Soft.*, vol. 39, no. 2, Feb. 2013. DOI: https://doi.org/10.1145/2427023.2427031

[19] D.H. Bailey, J.M. Borwein, "Crandall's computation of the incomplete Gamma function and the Hurwitz zeta function, with applications to Dirichlet L-series," *Applied Math. & Comp.*, vol. 268, pp 462-477, Jan. 2015. DOI: https://doi.org/10.1016/j.amc.2015.06.048

[20] R. Abergel, L. Moisan, "Fast and accurate evaluation of a generalized incomplete gamma function," *MAP5 2016-14*, pp 1-29, 2016. https://hal.archives-ouvertes.fr/hal-01329669.

[21] G.J.O. Jameson, "The incomplete gamma functions," *The Mathematical Gazette*, vol. 100, no. 548, pp. 298-306, Jul. 2016. DOI: https://doi.org/10.1017/mag.2016.67

[22] A. Gil, D. Ruiz-Antolín, J. Segura, N.M. Temme, "Algorithm 969: computation of the incomplete gamma function for negative values of the argument," *ACM Trans. Math. Soft. (TOMS)*, vol. 43, no. 3, pp. 1-28, Jan. 2017. DOI: https://doi.org/10.1145/2972951

[23] P. Greengard, V. Rokhlin, “An algorithm for the evaluation of the incomplete gamma function,” *Adv Comput. Math.*, pp 1-27, Mar. 2018. https://doi.org/10.1007/s10444-018-9604-x

[24] I. Progri, *Indoor Geolocation Systems—Theory and Applications*. *Vol. I*, 1st ed., Worcester, MA: Giftet Inc., ~800 pp., ~ 2023. (not yet available in print)

[25] I.S. Gradshteyn, I.M. Ryzhik, (A. Jeffrey, D. Zwillinger, editors) *Table of Integrals, Series, and Products*, 7th ed., Burlington, MA: Academic Press, 1171 pp., 2007.

[26] Anon, “Gamma function,” *Wikipedia, the free encyclopedia*, June 2022. https://en.wikipedia.org/wiki/Gamma_function

[27] Anon, “Incomplete Gamma function,” *Wikipedia, the free encyclopedia*, June 2022. https://en.wikipedia.org/wiki/Incomplete_gamma_functio n

[28] Anon, “Hypergeometric function,” *Wikipedia, the free encyclopedia*, June 2022. https://en.wikipedia.org/wiki/Hypergeometric_function

[29] Anon, “MATLAB 2022b,” *The MathWorks, Inc.*, Natick, MA, Copyright © 1994-2022, The MathWorks, Inc. https://www.mathworks.com/products/new_products/r20 22b-transition.html?s_tid=srchtitle_release2022b_2

[30] Anon., “Jack Nicklaus,” *Wikipedia, the free encyclopedia*, Oct. 2021. https://en.wikipedia.org/wiki/Jack_Nicklaus

[31] Anon., “Ronald Reagan,” *Wikipedia, the free encyclopedia*, June. 2022. https://en.wikipedia.org/wiki/Ronald_Reagan

8 Appendix A: Incomplete Gamma Function for Integer Values

There is so much that has already been published on the computation of the incomplete gamma function [13]-[28].

From the definition of the incomplete gamma function we have

$$\gamma(\alpha,x)=\int_0^x t^{\alpha-1}e^{-t}dt$$

$$=\frac{x^\alpha}{\alpha}\Phi(\alpha,1+\alpha;-x)$$

$$=\frac{x^\alpha e^{-x}}{\alpha}\Phi(1,1+\alpha;x) \tag{27}$$

Now, let us split the integral into two integrals:

$$\gamma(\alpha,x)=\int_0^b t^{\alpha-1}e^{-t}dt+\int_b^x t^{\alpha-1}e^{-t}dt$$

$$=\gamma(\alpha,b)+\int_b^x t^{\alpha-1}e^{-t}dt$$

$$=\gamma(\alpha,b)+\Delta\gamma(\alpha,b,x) \tag{28}$$

If we make the substitution (see Progri (2018, Sect. 3 pg. 56 [3])) for calculating (10) for values of $x\geq b$ we have the following

$$t'=e^{-t}\Rightarrow t=-\log(t')\Rightarrow dt=-\frac{dt'}{t'} \tag{29}$$

When

$$t\rightarrow|_b^x\Rightarrow t'\rightarrow|_{e^{-b}}^{e^{-x}} \tag{30}$$

Substituting (12) and (13) into the integral of (28) yields

$$\int_b^x t^{\alpha-1}e^{-t}dt=\int_{e^{-x}}^{e^{-b}}\log^{\alpha-1}(t')dt' \tag{31}$$

The solution of (31) for integer values of the parameter α can be obtained from Gradshteyn, Ryzhik (2007, 2.71, 2.711 pg. 237 [25]) as follows

$$\int_b^x t^{\alpha-1}e^{-td}dt=\int_{e^{-xd}}^{e^{-bd}}\log^{\alpha-1}(t')dt'\ \mathrm{x}$$

$$=\sum_{n=0}^{\alpha-1}\frac{(\alpha-1)(\alpha-2)\cdots(\alpha-n)t'\log^{\alpha-1-n}(t')}{(-1)^{\alpha-n-1}}\Big|_{e^{-x}}^{e^{-b}}\mathrm{xi}$$

$$=\sum_{n=0}^{\alpha-1}\frac{(\alpha-1)\cdots(\alpha-n)\left[\frac{\log^{\alpha-1-n}(e^{-b})}{e^b}-\frac{\log^{\alpha-1-n}(e^{-x})}{e^x}\right]}{(-1)^{\alpha-n-1}}$$

$$=\sum_{n=0}^{\alpha-1}(\alpha-1)(\alpha-2)\cdots(\alpha-n)\left|\begin{matrix}\frac{b^{\alpha-1-n}}{e^b}-\\ \frac{x^{\alpha-1-n}}{e^x}\end{matrix}\right.$$

$$=\sum_{n=0}^{\alpha-1}\binom{\alpha-1}{n}n!\left(\frac{b^{\alpha-1-n}}{e^b}-\frac{x^{\alpha-1-n}}{e^x}\right)$$

$$=\frac{b^{\alpha-1}\sum_{n=0}^{\alpha-1}\binom{\alpha-1}{n}n!b^{-n}}{e^b}-\frac{x^{\alpha-1}\sum_{n=0}^{\alpha-1}\binom{\alpha-1}{n}n!x^{-n}}{e^x} \tag{32}$$

Substituting (32) into the integral of (28) yields

$$\Delta\gamma(\alpha,b,x)=\left|\begin{matrix}e^{-b}b^{\alpha-1}\sum_{n=0}^{\alpha-1}\binom{\alpha-1}{n}n!\,b^{-n}-\\ e^{-x}x^{\alpha-1}\sum_{n=0}^{\alpha-1}\binom{\alpha-1}{n}n!\,x^{-n}\end{matrix}\right. \tag{33}$$

Next, let us write the solution of (33) using the confluent hypergeometric function formulation

$$\frac{x^\alpha\Phi(\alpha,1+\alpha;-x)}{\alpha}=\frac{b^\alpha\Phi(\alpha,1+\alpha;-b)}{\alpha}+\Delta\gamma(\alpha,b,x) \tag{34}$$

Which is equivalent with

$$\frac{x^{\alpha}\Phi(1,1+\alpha;x)}{\alpha e^{x}} = \frac{x^{\alpha}\Phi(1,1+\alpha;x)}{\alpha e^{x}} + \Delta\gamma(\alpha,b,x) \tag{35}$$

The reduction formulae (33)-(35) are analogous to other published material. For example, from Gradshteyn, Ryzhik (2007, 8.351 1. pg. 889 [25]) we have

$$\gamma(\alpha,b) = (\alpha-1)!\left[1 - e^{-b}\sum_{m=0}^{\alpha-1}\frac{b^m}{m!}\right] \tag{36}$$

$$\gamma(\alpha,x) = (\alpha-1)!\left[1 - e^{-x}\sum_{m=0}^{\alpha-1}\frac{x^m}{m!}\right] \tag{37}$$

If we take the difference of (37) with (36) we have

$$\Delta\gamma(\alpha,b,x) = (\alpha-1)!\left[e^{-b}\sum_{m=0}^{\alpha-1}\frac{b^m}{m!} - e^{-x}\sum_{m=0}^{\alpha-1}\frac{x^m}{m!}\right] \tag{38}$$

If we make the substitution

$$n = \alpha - 1 - m \tag{39}$$

Then we have

$$\Delta\gamma(\alpha,b,x) = (\alpha-1)!\left|\begin{matrix} e^{-b}\sum_{n=0}^{\alpha-1}\frac{b^{\alpha-1-n}}{(\alpha-1-n)!} - \\ e^{-x}\sum_{n=0}^{\alpha-1}\frac{x^{\alpha-1-n}}{(\alpha-1-n)!}\end{matrix}\right.$$

$$= \left|\begin{matrix} e^{-b}\sum_{n=0}^{\alpha-1}\frac{(\alpha-1)!b^{\alpha-1-n}}{(\alpha-1-n)!} - \\ e^{-x}\sum_{n=0}^{\alpha-1}\frac{(\alpha-1)!x^{\alpha-1-n}}{(\alpha-1-n)!}\end{matrix}\right.$$

$$= \left|\begin{matrix} e^{-b}b^{\alpha-1}\sum_{n=0}^{\alpha-1}\binom{\alpha-1}{n}n!\,b^{-n} - \\ e^{-x}x^{\alpha-1}\sum_{n=0}^{\alpha-1}\binom{\alpha-1}{n}n!\,x^{\alpha-1-n}\end{matrix}\right. \tag{40}$$

Even though (40) and (38) are equivalent, (40) is numerically more accurate because we have avoided the computation of very large numbers.

Next, another useful expression for the incomplete gamma function for integer values of the parameter α making use of the substitution (39) is as follows:

$$\gamma(\alpha,x) = (\alpha-1)!\left[1 - e^{-x}\sum_{n=0}^{\alpha-1}\frac{x^{\alpha-1-n}}{(\alpha-1-n)!}\right]$$

$$= (\alpha-1)!\left[1 - e^{-x}x^{\alpha-1}\sum_{n=0}^{\alpha-1}\frac{x^{-n}}{(\alpha-1-n)!}\right]$$

$$= (\alpha-1)!\left[1 - \frac{e^{-x}x^{\alpha-1}}{(\alpha-1)!}\sum_{n=0}^{\alpha-1}\binom{\alpha-1}{n}n!\,x^{-n}\right] \tag{41}$$

From (41) we have obtained two equivalent expressions for the computation of the incomplete gamma function for integer values of the parameter α: (for small values of the variable $0 \le x \le b$

$$\gamma(\alpha,x) = (\alpha-1)!\left[1 - \frac{e^{-x}}{(\alpha-1)!}\sum_{n=0}^{\alpha-1}\binom{\alpha-1}{n}n!\,x^{\alpha-1-n}\right] \tag{42}$$

For larger values of $b \le x < \infty$

$$\gamma(\alpha,x) = (\alpha-1)!\left[1 - \frac{e^{-x}x^{\alpha-1}}{(\alpha-1)!}\sum_{n=0}^{\alpha-1}\binom{\alpha-1}{n}n!\,x^{-n}\right] \tag{43}$$

Let us consider a few examples:

First, if we set $\alpha = 1$ in (33) we have a very simple solution of the difference of two exponential functions

$$\Delta\gamma(\alpha = 1,b,x) = e^{-b} - e^{-x} \tag{44}$$

From [27] Special values Sect. we have

$$\gamma(\alpha = 1,b) = 1 - e^{-b} \tag{45}$$

$$\gamma(\alpha = 1,x) = 1 - e^{-x} \tag{46}$$

It is straightforward to arrive at (36) if we take the difference of (38) with (37).

Second, if we set $\alpha = 2$ in (33) we have

$$\Delta\gamma(\alpha = 2,b,x) = 2[e^{-b}(b+1) - e^{-x}(x+1)] \tag{47}$$

An equivalent expression can be derived from Gradshteyn, Ryzhik (2007, 8.351 1. pg. 889 [25]).

This concludes the derivations of incomplete Gamma function for integer values of the parameter α.

---

i Progri L function is a function named after my mother Lumturi Progri. I have not given a lot of credit to my mother for her support throughout the later years of my life Because the landmark computation of the landmark computation of GBFD1K was really intended for larger values of the variable, the older I get the more I realize how lucky I am and how wonderful a mother I have, and how fitting it is to name landmark solution after my mother.

ii These fine, simplification, implementation details to enable the computation of the Kampé de Fériet functions K_1, K_2 that are not disclosed in this publication. There is a simple explanation because some details are meant to be kept private information.

iii For integer values of a parameter. I regret that it took me nearly six years to arrive at the landmark publication since, I had all the tools derived in Progri (2016, [3]) and in Progri (2018, [5]). This is because I underestimated my work and I overly relied on the current publications of the computation of the incomplete gamma function. Often, people arrive at landmark solutions when they have tried and have failed at everything else. In this case, I exhausted the computation of the generalized Bessel function distribution cdf of the first kind. There was only one thing that was left to do, and that was to look for a different solution. And this is how the landmark computation of the generalized Bessel function distribution cdf of the first kind was conceived.

iv In Progri (2016, [3]) I derived two sets of formulas side by side. The second set of formulas were derived by the transformation $y = e^{-x}$ because they were intended for large value of the variable x. Although a transformation will analytically produce identical formulas, numerically they will not be identical (unlike the elementary functions), which is the main reason why certain transformations are needed to produce equations that are intended for certain values of the variable x. This journal paper is in fact the best example to illustrate why this transformation of $y = e^{-x}$ leads to equations that are numerically fast and accurate.

v There was a typo in Gradshteyn, Ryzhik (2007, 2.71, 2.711 pg. 237 [25]). The correct solution is

$$\int_b^x t^{\alpha}e^{-td}dt = \frac{\int_{e^{-xd}}^{e^{-bd}}\log^{\alpha}(t')dt'}{d^{\alpha'}}$$

$$= \frac{\sum_{n=0}^{\alpha}(-1)^{n-\alpha}\alpha(\alpha-1)\cdots(\alpha-n+1)t'\log^{\alpha-n}(t')|_{e^{-xd}}^{e^{-bd}}}{d^{\alpha'}} \quad (1)$$

If we set $\alpha = 0$ from the lefthand side, we have

$$\int_b^x e^{-td}dt = \frac{-1}{d}\int_b^x e^{-td}d(-td)$$
$$= \frac{-1}{d}e^{-td}|_b^x$$
$$= \frac{e^{-bd}-e^{-xd}}{d} \quad (2)$$

However, from the righthand side of (1) we have

$$\frac{t'|_{e^{-xd}}^{e^{-bd}}}{d} = \frac{\int_{e^{-xd}}^{e^{-bd}} dt'}{d}$$
$$= \frac{e^{-bd}-e^{-xd}}{d} \quad (3)$$

If we set $\alpha = 1$ from the lefthand side, we have if we do integration by parts

$$\int_b^x te^{-td}dt = t\left.\frac{e^{-td}}{-d}\right|_b^x - \frac{(-1)^2}{d^2}\int_b^x e^{-td}d(-td)$$
$$= \frac{be^{-bd}-xe^{-xd}}{d} - \frac{e^{-bd}-e^{-xd}}{d^2} \quad (4)$$

However, from the righthand side of (1) we have

$$\int_b^x t^{\alpha}e^{-td}dt = \frac{\int_{e^{-xd}}^{e^{-bd}}\log\left(t'\right)dt'}{d^2}$$
$$= -\frac{t'\log(t')|_{e^{-xd}}^{e^{-bd}}}{d^2} - \frac{e^{-bd}-e^{-xd}}{d^2}$$
$$= \frac{bde^{-bd}-xde^{-xd}}{d^2} - \frac{e^{-bd}-e^{-xd}}{d^2}$$
$$= \frac{be^{-bd}-xe^{-xd}}{d} - \frac{e^{-bd}-e^{-xd}}{d^2} \quad (5)$$

Since (2) and (3) are identical and (4) and (5) are identical; hence, there is a typo (1) in Gradshteyn, Ryzhik (2007, 2.71, 2.711 pg. 237 [25]). The $(-1)^k$ should be $(-1)^{k-m}$.

Moreover, this solution only exists if and only if $b > 0$.

[vi] Modifications of this equation is required for non-integer values of the parameter p is required. Because this is significantly new work it will be published in a new journal paper.

[vii] An equivalent expression can be obtained based on derivations in Appendix A from Gradshteyn, Ryzhik (2007, 8.351 1. pg. 889 [25])

[viii] Ditto i.

[ix] There is a false impression that only the research that is funded by the government bureaucrats is worthy of financial support, awards, & recognition. This is not to say that President Ronald Reagan wanted to demonize the role of the government as an enterprise, or resource, or originator of many inventions. But, when the government spending is abused for wasteful spending of the taxpayers trillions of $ dollars, and moreover, when it controls and suppresses innovation and ignores or completely denies funding to innovators and incubators based on political beliefs, then said President Ronald Reagan this type of government is the problem.

[x] Ditto v.

[xi] Ditto vi.